Molecular-dynamics study of lattice-defect-nucleated melting in silicon

S. R. Phillpot, J. F. Lutsko, D. Wolf, and S. Yip*
Materials Science Division, Argonne National Laboratory, Argonne, Illinois 60439
(Received 20 January 1989)

The high-temperature behavior of both a high-angle twist grain boundary and a free surface on the (110) plane of silicon are investigated using molecular dynamics and the Stillinger-Weber potential. It is found that, above the thermodynamic melting point, melting is nucleated at the grain boundary or surface and propagates through the system with a velocity that increases with temperature. We conclude that, due to the relatively fast nucleation times, melting in real crystals should be initiated at grain boundaries and surfaces, a conclusion that is entirely in accord with experiment.

I. INTRODUCTION

While there is no question about the thermodynamic significance of melting, the mechanistic aspects of how the transition occurs are still not completely understood. In a general discussion of melting, one should distinguish at the outset between intrinsic and extrinsic defects. Whereas an intrinsic defect is produced thermally, an extrinsic defect results from external action, including the introduction of surfaces in creating a finite crystal. There exists a number of theoretical models, each attempting to describe how a collection of atoms in a crystalline arrangement becomes unstable against a liquid configuration. All of these models consider only the effects of intrinsic defects. An early model, due to Lindemann, treats melting as a vibrational instability.[1] Later it was suggested that the transition is caused by a lattice-shear instability,[2] the catastrophic generation of dislocations,[3] or the presence of thermal vacancies and other point defects.[4] Since direct experimental evidence in support of each of these models is not definitive, the question of the predominant initiation mechanism of melting remains.

In contrast to the assumptions of the above theories, it is well known that melting of a solid generally proceeds from the surface. For example, it was observed in measurements on silica[5] and phosphorus pentoxide[6] that melting was not a homogeneous process; invariably it occurred at free surfaces and grain boundaries. A variety of experimental data now exist which point to the controlling role of an extrinsic surface.[7] Small atomic clusters, with a significant fraction of the particles on or close to the surface, have been observed to exhibit quite different melting behavior from that of the bulk substance; for example, melting-point depression up to 30% has been measured in metal clusters of a diameter of 20–30 Å,[8] as has substantial superheating of argon bubbles of similar size formed in an aluminum lattice,[9] and of hydrogen bubbles in amorphous silicon.[10] Superheating also has been measured recently in small single crystals of silver coated with gold, the latter with a higher melting point.[11] The implication of these results is that while melting is a thermodynamic transition, in general it is physically initiated at either an external surface or an internal interface such as a grain boundary or a dislocation.

The difficulty in the experimental test of melting theories primarily stems from an inability to directly observe the phenomenon in sufficient atomistic detail, particularly with processes occurring in the bulk. Lack of atomistic detail is not a problem with molecular dynamics (MD) (Ref. 12) and Monte Carlo[13] simulations, techniques with unique capabilities for elucidating the thermal behavior of bulk matter. There exist a number of simulation studies of melting and freezing phenomena,[13,14–18] including various aspects of the dislocation theory of melting[3] and, more recently, disordering and melting of aluminum surfaces.[18]

Aside from the problem of bulk melting, melting at a free surface is itself of considerable current interest. Surface melting has been directly observed by scattering protons from an atomically clean Pb(110) surface,[19] the process occurring at approximately $0.75T_m$, T_m being the bulk melting point. The transition begins with partial disordering of the surface region and progresses to a completely disordered film whose thickness increases rapidly as the temperature approaches T_m. These data provide support for the theoretical prediction that the thickness of the surface layer should diverge like $\ln[T_0/(T_m-T_0)]$, where T_0 is the difference T_m-T at which the disordered film is first formed.[20] Surface disordering and melting in various model systems have been studied by molecular dynamics.[16–18] For example, melting of the (111) and (100) surfaces of silicon induced by laser-pulse heating[17] and surface disordering on (110) and (111) surfaces of aluminum at temperatures below bulk melting have been simulated with use of rather sophisticated potential functions.[18]

The problem of melting at a grain boundary (GB), which has long been of interest in the metallurgical literature,[21] has also attracted attention from the simulation community recently. A central question has arisen concerning the structural stability of grain boundaries in metals at elevated temperatures, because the findings from different molecular-dynamics studies appear to be inconsistent. While in all the simulations the GB core becomes appreciably disordered, beginning around $0.5T_m$, the issue is whether it remains crystalline up to T_m (Ref. 22) or undergoes local melting at a temperature distinctly below T_m (so-called premelting).[23,24] A direct free-energy

calculation has suggested that the behavior, where the crystalline boundaries are replaced by highly disordered, liquidlike layers, corresponds to a phase transition which appears to be of first order;[25] another study, also based on the analysis of free energies, indicates that melting at the grain boundary is not a true phase transition, that thermodynamic parameters should be continuous, and that the quasiliquid layer must retain some crystalline symmetry.[26] Moreover, it was suggested that there can be superheating in certain boundaries.[26]

The simulation results which indicate high-temperature disordering (including premelting) have not been confirmed in experiments. Instead, measurements on copper using the technique of rotating sphere-on-a-plate indicate an absence of premelting up to $0.95T_m$ to $0.99T_m$ (Refs. 27 and 28), and transmission electron spectroscopy results on aluminum bicrystals showed no boundary melting up to $0.999T_m$.[29] The experimental conclusion thus far is that complete grain-boundary melting, in the sense of the boundary being replaced with a liquid layer of several atomic diameters, is not observed below T_m. This interpretation does not rule out a significantly disordered boundary which still retains the essential crystalline order in the two grains adjoining the boundary slab.[29,30] As for superheating, while it has been observed in molecular solids,[5,6] in bulk metallic solids it is possible only under very special and limited conditions.[11]

In discussing simulation results on melting it is important to keep in mind what is meant by the melting point since this term has been used for different quantities. There are three quantities, all of which have been called the melting point: the known experimental melting point of the substance being simulated, the thermodynamic melting point of the simulation model, T_m, which depends on the potential used, and the mechanical instability of the model which also depends on the potential. Strictly speaking, independent of whether it agrees numerically with T_m, the experimental melting point has nothing to do with the model and therefore should not be used in evaluating model behavior. As for T_m, it is the true melting point, defined as the temperature at which the solid and liquid free energies cross (operationally there can be other ways of determining T_m as we will show below). In most simulations to date the free-energy calculation has not been carried out; what is sometimes taken as the melting point is an approximation to T_s, the temperature at which a single crystal with the same potential and three-dimensional (3D) periodic-border conditions (3D PBC's) becomes unstable upon heating. The difference between T_s and T_m is the range in which the model solid can be superheated; in certain simulation models this range can be a significant fraction of T_m.

The prime purpose of the present pair of papers is to investigate the role of an extrinsic surface on melting by molecular-dynamics simulation. A secondary motivation is to contribute to the resolution of the GB premelting debate. Melting in silicon in the presence of a grain boundary and of a free surface is studied in this paper, and the effects of a grain boundary, free surface, and a void on melting in a metal are treated in the following paper.[31] We find that in all cases melting is initiated at the extrinsic defect, and that by taking advantage of the ability of simulation to follow the melting process under superheating one can determine the thermodynamic melting point of the model, T_m, without performing a free-energy calculation, which is a nontrivial task, as will be discussed in the following paper.

The present results on melting behavior in a grain boundary are particularly relevant to the issue of GB premelting. In a recent MD investigation of the high-temperature stability of metal GB's, a close connection between GB migration and the onset of thermal disordering near the interface was observed.[32] It was pointed out that in all the previous simulations which showed a premelting or disordering transition, the center of mass of the bicrystal had been kept fixed, thus artificially constraining the relative motion of the two halves of the bicrystal parallel to the GB plane (GB sliding). When this constraint was removed, the disorder observed was found to be merely a transient intermediate state formed during the sliding and subsequent migration of the GB from one plane to the next.[32] Because we wish to investigate the disordering associated with melting, it is desirable to eliminate the effect of GB migration. Silicon is a good choice for this study because the GB mobility in undoped Si is known to be much lower than that in metals.[33] Also, an empirical potential suitable for simulations has been presented by Stillinger and Weber (SW);[34] it has proved to be quite successful in recent studies on the bulk crystal,[34,35] the liquid,[34,35] the crystal-liquid interface,[36,37] and grain boundaries.[38]

In the next section we describe the computational methods used in simulating a silicon bicrystal model of a high-angle twist boundary and a single-crystal model with free (110) surfaces. Results on the superheating of the bicrystal are presented in Sec. III. The results of a corresponding study on the (110) free surface are given in Sec. IV. In Sec. V we comment on the significance of our results in the context of initiation mechanisms for melting and of GB premelting. A less detailed discussion of the results of GB-nucleated melting have appeared previously.[39]

II. SIMULATION MODELS AND METHOD

In this section we describe several aspects of our simulation method which are essential for the appreciation of the results to be presented. These include the use of a recently developed border condition,[40] the selection of a GB geometry, and the implementation of data analysis procedures capable of detecting the spreading of a melted zone. We also briefly describe the SW potential used in this study.

A. Border condition for bicrystal simulations

In simulation studies of GB's a technical problem arises in the implementation of border conditions on the simulation cell which properly represent the effects of the medium beyond the cell. For coherent GB's there is no

difficulty in the two directions parallel to the interfacial plane since 2D periodic-border conditions (2D PBC's) should be used to take advantage of the symmetry of the coincidence-site-lattice models of grain boundaries.[40] In the direction normal to the plane, periodic[22,23,26] and fixed-border[24] conditions have been used but are considered unsatisfactory because of the unphysical effects induced in the system response, particularly at high temperatures. Recently a new border condition has been proposed which introduces movable perfect-crystal blocks at the two ends of the simulation cell.[40] The present simulation makes use of this new method.

Figure 1 shows the simulation cell consisting of two regions, a region I in which the atoms move according to the Newtonian equations of motion and a region II consisting of two rigid blocks of atoms. The cell is periodic in the x and y directions. The extent of the blocks in the z direction is determined by the range (i.e., cutoff radius) of the potential, and initially, the positions of the rigid blocks are fixed by taking the distance between the outermost plane of region I and the first plane of the corresponding rigid block to be the perfect-crystal interplanar spacing appropriate for the simulation temperature. Such a region I–region II strategy is commonly used in the zero-temperature (lattice-statics) simulation of grain boundaries.[41,42]

This border condition specifies how the rigid blocks move during the simulation. Conceptually the movement of the rigid blocks in the z direction is treated differently from their translations parallel to the interface plane. The z-direction movement is treated by applying a modified Parrinello-Rahman scheme,[43] whereas each block translates in the x-y plane as a single particle with an effective mass. Thus, while the movement in z is governed by the *pressure* exerted on the rigid blocks by region I, the sliding of each block in the x-y plane is controlled by the *force* exerted on the block across the border of the two regions.

While we allow expansions and contractions of the simulation cell along the z direction, we do not allow areal expansions or contractions (in the x-y plane), when simulating an isolated interface embedded in bulk crystal. Therefore, the x-y dimensions of our simulation cell are fixed by the lattice parameter of the bulk region. This lattice parameter is an input parameter to our simulations; it is determined independently from a constant-pressure simulation of a bulk ideal crystal (with 3D periodic borders) at the desired temperature for the same interatomic potential.

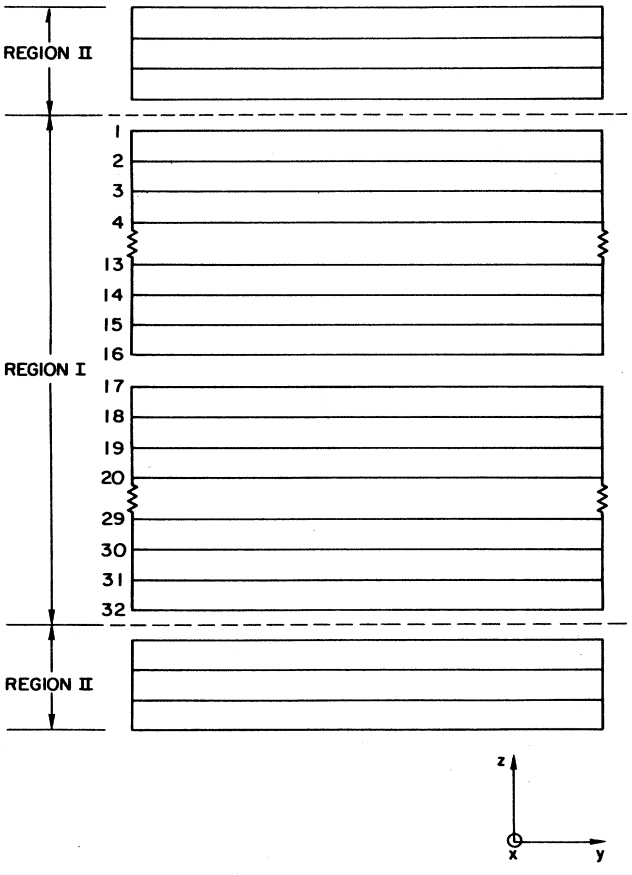

FIG. 1. Schematic of our simulational cell. Region I contains 32 planes with 22 atoms in each plane. Initially the GB lies between planes 16 and 17.

B. Geometries of the GB and surface

The GB chosen for this study is the so-called $\Sigma 11$ (110) high-angle twist boundary. This is a boundary on the (110) plane obtained by rotating two perfect semicrystals with (110) faces by $\theta = 50.48°$ about the plane normal. The area of the rectangular planar unit cell is $\Sigma = 11$ times that of the corresponding primitive planar unit cell ($\Sigma = 1$) on the (110) plane; each lattice plane thus contains 22 atoms. Our computational cell was chosen to contain 32 (110) planes; therefore there are 704 atoms in region I.

The primary considerations underlying the present choice of GB geometry are (a) its relatively large planar unit cell (thus representing what we consider a "typical" high-angle GB), (b) the large spacing of lattice planes parallel to the GB plane [$d(110) = 0.3lla_0$, where a_0 is the lattice parameter], and (c) the relative insensitivity of its energy towards translations parallel to the GB plane. Because of (b) behavior of atoms within an individual plane can be isolated from that of the others. The zero-temperature structure and energy of this boundary were investigated in Ref. 38.

To study free surfaces, we use an ideal crystal of the same unit-cell dimensions, area, and number of atoms as the bicrystal, but without the interface. A pair of free surfaces is introduced by removing both region-II rigid blocks. Previous simulations have made use of a fixed substrate, thereby producing a single free surface (see for example, Refs. 17 and 18); this would correspond to the removal of only one of the region-II rigid blocks. We prefer to have two free surfaces in the computational cell as they provide twice as much data, thereby reducing statistical errors.

In the present geometry the free surfaces are initially

separated by 32 lattice planes, which we find is sufficiently far to ensure that they do not interact significantly over the duration of the simulations (≈ 23 ps). If we were modeling a thin film, the x-y dimensions of the simulation cell also would be allowed to change dynamically. However, here we are modeling a free surface on a bulk substrate; therefore, the x-y dimensions are those of the bulk ideal crystal appropriate for the simulation temperature, as in the GB simulations. Because the volume of a system with free surfaces can change dynamically without using a constant-pressure scheme, these simulations are performed at constant volume.

C. Characterization of planar disorder and melting

Typically in MD simulations the information contained in the detailed atom trajectories is condensed into standard thermodynamic and structural quantities, such as temperature, internal energy, and mean-square displacement (MSD). However, one should calculate additional properties, which particularly probe the phenomenon of interest. Here we are principally interested in monitoring the thermal disordering induced by the presence of a grain boundary or a surface. Because both of these are planar defects, it is essential to monitor spatial variations of the relevant properties along the normal to the interface plane. To obtain such information, we divide region I into slices along the z direction. Here each slice is chosen to contain a single atomic (110) plane in the crystal. As our results show, such a slicing scheme also provides useful information about melted regions.

To investigate the breakdown of crystalline order upon melting, we define the square of the magnitude of the static structure factor, $S(\mathbf{k})$, which for brevity we denote simply by $S^2(\mathbf{k})$:

$$S^2(\mathbf{k}) \equiv |S(\mathbf{k})|^2 = \left[\frac{1}{N}\sum_{i=1}^{N}\cos(\mathbf{k}\cdot\mathbf{q}_i)\right]^2 + \left[\frac{1}{N}\sum_{i=1}^{N}\sin(\mathbf{k}\cdot\mathbf{q}_i)\right]^2 , \quad (1)$$

where $\mathbf{q}_i$ is the position of atom i. For the *overall* $S^2(\mathbf{k})$, all the atoms in the simulation cell are included in the sums in Eq. (1), whereas for the *planar* structure factor, $S_p^2(\mathbf{k})$, only atoms in a given lattice plane are considered. For an ideal crystal at zero temperature, $S_p^2(\mathbf{k})$ then equals unity for any wave vector $\mathbf{k}$ which is a reciprocal lattice vector in the plane p. By contrast, in the liquid state (without long-range order in plane p), $S_p^2(\mathbf{k})$ fluctuates near zero. As the two halves of the bicrystal are rotated with respect to each other about the GB-plane normal two different wave vectors, $\mathbf{k}_1$ and $\mathbf{k}_2$, are required, each corresponding to a principal direction in the related half. For a well-defined crystalline lattice plane, say in semicrystal 1, $S_p^2(\mathbf{k}_1)$ then fluctuates near a finite value (≈ 1) appropriate for that temperature whereas $S_p^2(\mathbf{k}_2)\approx 0$. In the GB region, due to the local disorder, one expects somewhat lower values for $S_p^2(\mathbf{k}_1)$. By monitoring $S_p^2(\mathbf{k}_1)$ and $S_p^2(\mathbf{k}_2)$ every slice may be characterized as (a) belonging to semicrystal 1 [for $S_p^2(\mathbf{k}_1)$ finite, $S_p^2(\mathbf{k}_2)\approx 0$], (b) belonging to semicrystal 2 [for $S_p^2(\mathbf{k}_1)\approx 0$, $S_p^2(\mathbf{k}_2)$ finite], or (c) disordered or liquid [for $S_p^2(\mathbf{k}_1)\approx 0$, $S_p^2(\mathbf{k}_2)\approx 0$]. The vectors $\mathbf{k}_1$ and $\mathbf{k}_2$ were chosen to represent reciprocal lattice vectors in the $\langle 110\rangle$ direction in each half of the bicrystal. For the free-surface calculations only a single value of $\mathbf{k}$ was used; this too was chosen to be in a $\langle 110\rangle$ direction.

As a further measure of the overall disorder in the system, we introduce the quantity N_{def} which represents the number of defected atoms. An atom is considered defected if its number of nearest neighbors is not equal to the ideal-crystal coordination number. We have defined the nearest-neighbor shell to end at $0.577a_0$, which is halfway between the ideal-crystal first- and second-nearest-neighbor distances. In this definition the value of N_{def} is zero for an ideal crystal, even at elevated temperatures. For a liquid, on the other hand, the value of N_{def} is equal to the number of atoms in the system. For the case of silicon this can be seen from the liquid radial distribution function calculated at ≈ 1975 K,[34] in which the coordination out to $0.63a_0$ was given to be 8.07. From this we estimate that the coordination is ≈ 7 out to $0.577a_0$, the distance used in our calculation of N_{def}. Although at lower temperatures, the coordination may be expected to be somewhat less, since the coordination of ideal-crystal silicon is 4, we expect that all atoms in the liquid will be defected at the temperatures considered here.

D. The Stillinger-Weber potential

No two-body potential has been found to stabilize the diamond lattice: a potential containing interactions amongst three or more atoms is required. A number of potentials for silicon have been proposed in recent years.[34,44–46] Stillinger and Weber[34] (SW) have introduced a potential containing both two- and three-body components. The two-body part increases strongly at small atomic separations, has a minimum at the nearest neighbor distance, a_0, and goes smoothly to zero at a distance d, which is a little less than the zero-temperature ideal-crystal second-nearest-neighbor distance. The three-body part has the form:

$$\Phi_3 \sim \sum_{i,j,k} \exp[\gamma/(r_{ij}-d)]\exp[\gamma/(r_{ik}-d)](\cos\theta_{jik}+\tfrac{1}{3})^2 , \quad (2)$$

where r_{ij} and r_{ik} are the lengths of the vectors joining particles i and j, and i and k, respectively, and γ is a constant. θ_{jik} is the angle between these vectors. Φ_3 is zero for ideal tetrahedral angles and positive otherwise.

The parameters of the SW potential were chosen to give the diamond lattice as the lowest-energy crystal structure, and to give both a reasonable value for the silicon melting temperature and reasonable agreement with the liquid radial distribution function observed experimentally.

The SW potential is particularly suitable for this study for two reasons. First, more than the other proposed potentials, its properties have been investigated and well characterized. In an exhaustive study of the phase dia-

gram obtained for the SW potential, Broughton and Li[35] have determined the thermodynamic melting temperature T_m by free-energy analysis of the bulk ideal crystal. They obtained a value $T_m = 1691 \pm 20$ K which is to be compared with the experimental value of 1683 K. Second, the SW potential has been successfully used to describe silicon in a wide variety of environments, ranging from small clusters[47] to grain boundaries,[38] to the amorphous phase.[48] Of particular relevance here are the studies of internal interfaces[36,37,49] and surfaces,[17] which show that the SW potential can model experimentally observed phenomena.

III. GRAIN-BOUNDARY INDUCED MELTING

Prior to the GB simulation a perfect 3D periodic crystal containing 216 particles was superheated. This system was found to melt at between 2400 and 2600 K, which is consistent with previous results.[34,35] We believe this is a good approximation of the mechanical melting temperature, T_s, which is considerably higher than the thermodynamic melting temperature, $T_m = 1691 \pm 20$ K.[35]

In all the simulations the time step was 1.15×10^{-15} s, for which energy was found to be conserved to six significant figures for simulations of several thousand time steps. At the beginning of each simulation run particles were given random velocities corresponding to a temperature of 1200 K. To reach the desired simulation temperature the system was then heated by 100 K every 200 time steps. As we are primarily interested in phase transitions which involve a latent heat, when the desired temperature was reached a thermostat was applied by rescaling the particle velocities. A typical simulation run extended to $\approx 18\,000$ time steps (≈ 21 ps) at the desired temperature. In the following discussion, all simulation times given exclude the time required for heating.

Our bicrystal simulations were performed at six different temperatures: 1650, 1750, 1800, 1900, 2000, and 2100 K. Although these temperatures are below T_s, we shall see that at all but the lowest temperature the system is unstable to melting nucleated at the GB.

Before discussing our results in detail, we point out that our border condition appeared to work quite well. As in the previous study of a Lennard-Jones solid,[40] even at the highest temperature simulated, no anomalies in the energy or dynamics of particles near the region I–region II interface were observed.

Figure 2 shows the plane-by-plane profile of the instantaneous planar structure factors, defined in Sec. II C above, after 9000 time steps at 1650 K. The sharp transition, over a width of only 2–3 (110) lattice planes, of $S_p^2(\mathbf{k}_1)$ between almost zero and unity, coupled with a corresponding decrease in $S_p^2(\mathbf{k}_2)$, demonstrates the existence of crystalline order in the entire bicrystal. A comparison of these results with those after the first 2000 time steps shows no increase in the width of the GB region nor a change in the location of the GB plane. The latter indicates that the GB is, indeed, immobile at that temperature during the entire simulation. The near-unity values of $S_p^2(\mathbf{k})$ away from the GB, even at elevated temperatures, reflect the relative stiffness of this covalent material. Corresponding to the stability of the bicrystal, reflected by these structure factors, the slice-by-slice potential energy and MSD were found to be time independent. Also the total number of defected atoms in the system did not change.

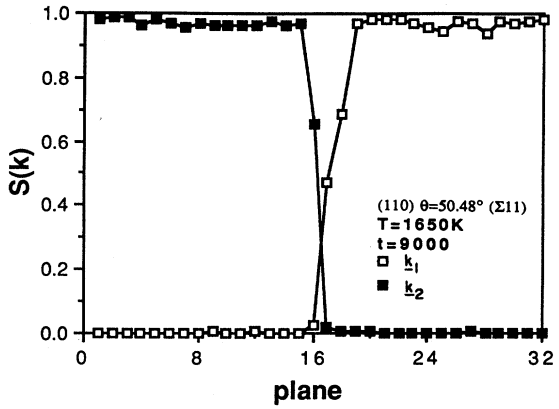

FIG. 2. Instantaneous values of $S_p^2(\mathbf{k}_1)$ and $S_p^2(\mathbf{k}_2)$ for the 32 slices parallel to the (110)Σ11 GB after 9000 time steps at 1650 K.

In contrast to the 1650-K simulation, the GB was found to be unstable at all higher temperatures investigated, 1750–2100 K; temperatures to which an ideal crystal can be superheated with no nucleation of the liquid. We find qualitatively the same behavior at all these temperatures. Thus in Figs. 3–6 only results obtained at $T = 1900$ K are summarized.

Figure 3 shows the instantaneous planar structure factors after 8600 and 17 600 time steps for the 1900-K simulation. They illustrate the spreading of a disordered region, initiated at the GB, into the two semicrystals. The width of this disordered region is defined as the number of planes in which both structure factors have a value of less than 0.5. Figure 4 shows that the width of this disordered region increases linearly in time, over the entire simulation interval. This gives a velocity of disordering for each of the two disordered-crystalline interfaces: $v_w(1900\text{ K}) = 39.5 \pm 5.5$ m/s.

Knowing the behavior of $S_p^2(\mathbf{k})$ is not sufficient to tell us whether the spreading disordered region is liquid, disordered but solid, or amorphous. One can look to the atomic mobility, as measured by the MSD, to make this distinction. Figure 5(a) shows a slice-by-slice analysis of the MSD for the system at 1900 K at the same two instants as in Figure 3. It is clear that both the width of the disordered region and the MSD of atoms in the region have increased. Figure 5(b) shows that the MSD of the two slices, taken from the center of the disordered region, attains a linear behavior that is characteristic of diffusive motion. Based on these data, we determine the diffusion constant to be $\approx 0.7 \times 10^{-8}$ m^2/s. This is comparable to the value found for the liquid at this temperature.[35] Thus the spreading region is indeed liquid.

The number of defected atoms, N_{def}, provides another way of characterizing the disordering of the system. Figure 6 shows that for $T = 1800$, 1900, 2000, and 2100 K,

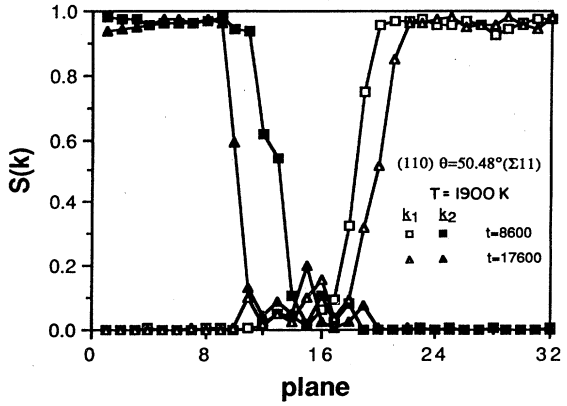

FIG. 3. Instantaneous values of $S_p^2(\mathbf{k}_1)$ and $S_p^2(\mathbf{k}_2)$ for the 32 slices parallel to the (110)Σ11 GB after 8600 (squares) and 17 600 time steps (triangles) at 1900 K.

after initial nucleation, N_{def} increases approximately linearly with time. (We note that although at 1750 K the system is clearly melting, the dynamics are too slow to extract reliable values for v_w and v_{def}.) These data also allow us to extract a propagation velocity, v_{def}, which we find to be $v_{\text{def}}(1900\text{ K}) = 28.1 \pm 5.3$ m/s.

In analogy to Fig. 6, Fig. 7 shows the time dependence of the width of the liquid region as determined via N_{def}. From these two figures we have determined the velocity-temperature relations, shown in Fig. 8. (The data used to generate this figure are given in Table I.) It can be seen that both relations show the velocity to decrease with decreasing temperature. We also note that at the higher temperatures v_w is significantly greater than v_{def}. As we shall discuss below this difference provides useful insights into the nucleation mechanism of melting.

The velocities in Fig. 8 are clearly related to the propagation velocity of the solid-liquid interface. If either v_{def} or v_w truly measures this velocity, then the extrapolated temperature T_0 at zero propagation velocity should be the temperature of liquid-solid coexistence; i.e., T_0 must be the thermodynamic melting temperature. From the results of our simulations we know T_0 to lie between 1650 K, at which the GB is stable, and 1750 K, at which the system is observed to melt. Because the data in Fig. 8 clearly do not lie on straight lines, a quadratic fit is used

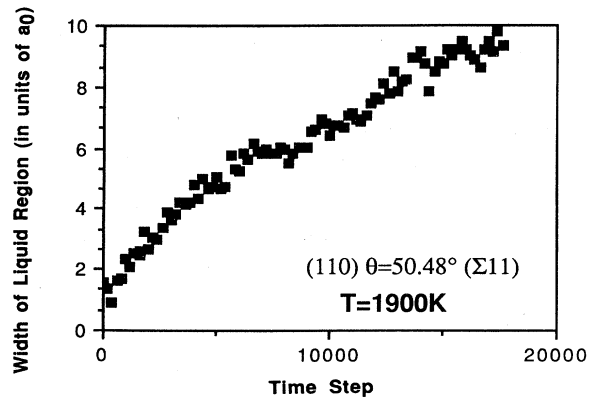

FIG. 4. Instantaneous width of the disordered region as a function of time at 1900 K. The width is defined as the number of planes in which both planar structure factors have a value of less than 0.5.

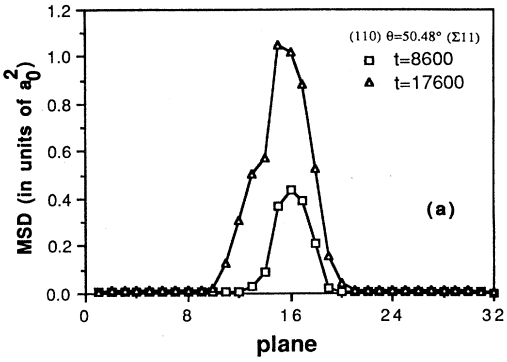

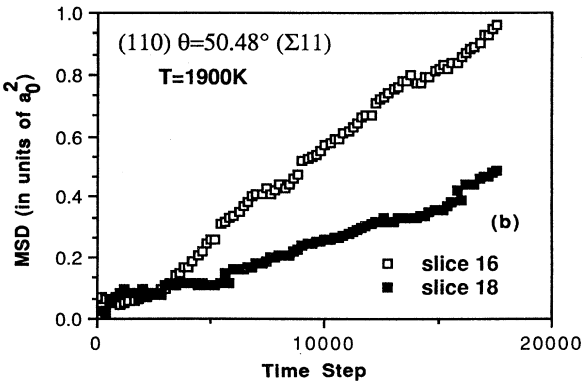

FIG. 5. (a) Instantaneous mean-square-displacement profile after 8600 and 17 600 time steps at 1900 K; (b) MSD vs time for slices 16 (open squares) and 18 (solid squares).

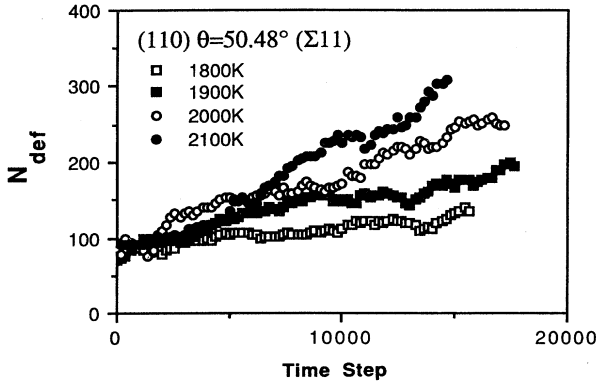

FIG. 6. Number of defected atoms in the bicrystal as a function of time for four temperatures.

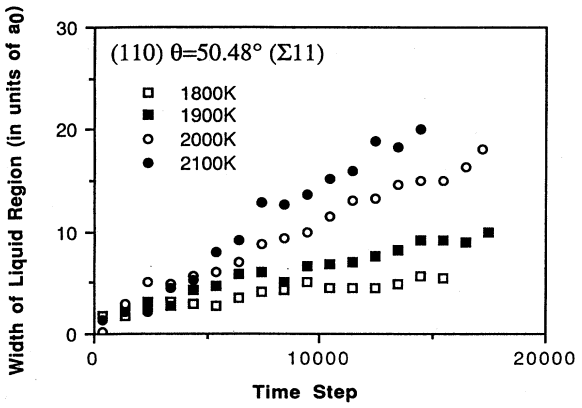

FIG. 7. Width of the GB, as determined from analysis of the planar structure factors, as a function of time at four temperatures.

for the extrapolation to zero velocity. For $v_{\rm def}$ this yields $T_0=1665\pm80$ K. A similar extrapolation of v_w to zero gives $T_0=1710\pm50$ K. [A similar extrapolation procedure has recently been used by Kluge and Ray[49] in their studies of melting and crystallization at Si(100) interfaces.] We regard it as significant that these two extrapolated temperatures agree within statistical errors. Furthermore, they also agree with the thermodynamic melting temperature, $T_m=1691\pm20$ K.[35] Therefore both $N_{\rm def}$ and the GB width, as characterized via $S(\mathbf{k})$, give consistent information, and we conclude that the propagation of the solid-liquid interface seen in all but the 1650-K GB simulations is due to ordinary thermodynamic melting of the bicrystal.

As we have noted v_w is significantly greater than $v_{\rm def}$ at high temperatures. This difference suggests that one may obtain some insight about the mechanism of melting from considering the simulation data in more detail. Three pertinent observations can be summarized as follows.

(i) Figure 9 shows the time dependence of the in-plane and out-of-planes MSD's for a single slice in the center of

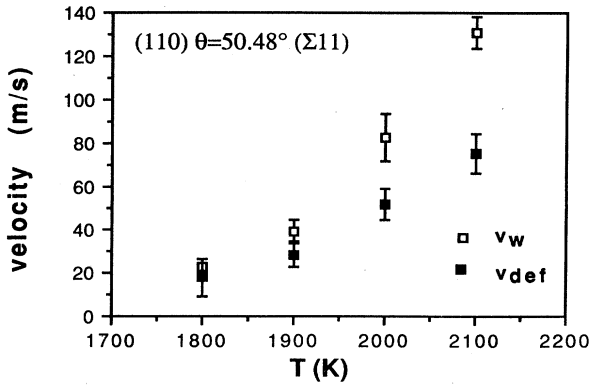

FIG. 8. Propagation velocities, $v_{\rm def}$ (solid squares) and v_w (open squares), as function of temperature.

TABLE I. Propagation velocity of the two solid-liquid interfaces for melting nucleated at a GB, as determined from an analysis of the GB width (v_w), from the change in density of the system (v_h), from the number of defected atoms ($v_{\rm def}$), and for surface nucleation as determined via the number of defected atoms ($v_{\rm def}$).

	Propagation velocity (m/s)			
	GB			Free surface
T (K)	v_w	v_h	$v_{\rm def}$	$v_{\rm def}$
1800	23±4	24±6	18±9	
1900	39±5	36±11	28±5	22±3
2000	83±10	84±11	52±7	56±6
2100	131±7	127±15	76±9	77±4
2200				95±2

the bicrystal. It can be seen that the in-plane disordering occurs first, and it is only after about 5000 time steps that atoms begin to move significantly out of the plane. Beyond ≈10 000 time steps the slopes of the two curves are similar, an indication that the liquid is fully isotropic.

(ii) Because silicon contracts on melting, the length h, of the computational cell should decrease with time. This decrease is approximately linear in time, as is shown in Fig. 10 for the 1900-K simulation. Analysis of $h(t)$ should allow us to extract a further propagation velocity, v_h, for the solid-liquid interface. To perform such a calculation, we need to assume that the entire density change produced on melting an ideal crystal under 3D PBC's at zero pressure is reflected in a corresponding change in h upon melting of the bicrystal.

At time $t=0$, the system is totally crystalline and has a length h_c. At a later time, t, $n(t)$ of the N atoms in the system are at the density of the liquid, and the length of the system is $h(t)$. If h_l denotes the length of the entirely liquid system then

$$h(t)=h_c+[n(t)/N](h_l-h_c)\ . \tag{3}$$

h_c is obtained from extrapolation to zero time in Fig. 10.

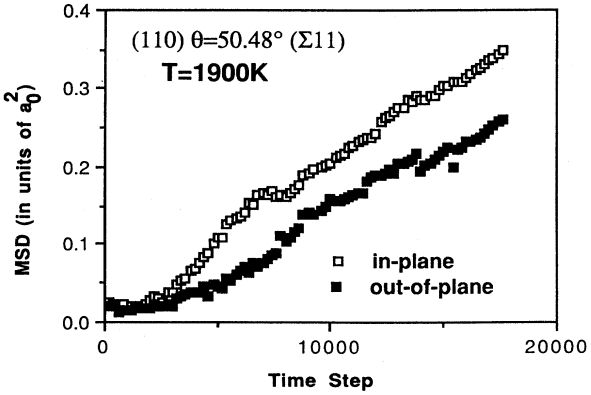

FIG. 9. Mean-square displacement parallel to (open squares) and perpendicular to the GB plane (solid squares) for a slice at the center of the liquid region as a function of time at 1900 K.

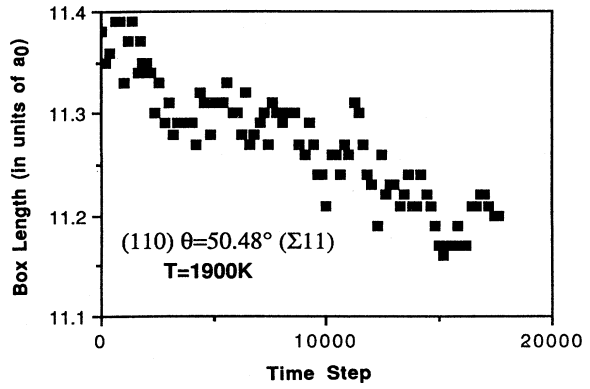

FIG. 10. Length of the bicrystal computational cell in the z direction (parallel to the GB-plane normal), as a function of time at 1900 K. The length of the cell at $T=0$K is $11.36a_0$. (a_0 is the $T=0$ lattice parameter.)

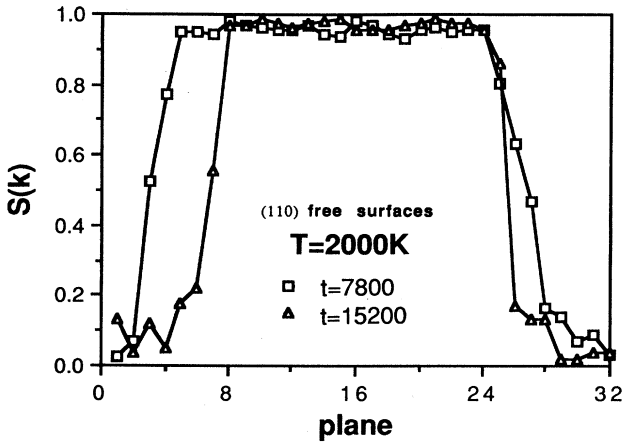

FIG. 11. Instantaneous value of $S_p^2(\mathbf{k})$ for the 32 slices parallel to the (110) free surfaces after 7800 and 15 200 time steps at 2000 K.

Then using the slope of a linear fit to Fig. 10 and the known densities of the solid and liquid at that temperature,[35] we can calculate $n(t)$. Hence, we can determine the velocities v_h. These are also shown in Table I. We note that at the two higher temperatures these values are significantly larger than v_{def} and are, within the error bars, equal to v_w.

(iii) The inequality between v_w and v_{def} seems to arise from the different degrees of disorder probed by the planar structure factor and the number of defected atoms. Because the in-plane structure factor is highly sensitive to even small deviations from ideal-crystal order, v_w may be expected to be at least as large as v_{def} which reflects the greater degree of disorder associated with a change of coordination.

Based on these three observations, we envisage melting as taking place by a two-stage process. In the first stage there is disordering, mainly amongst atoms within a single atomic plane, which involves no change in the coordination of the atoms. Because v_h is the same as v_w it appears that this disordering is accompanied by a density increase up to the density of the liquid. One is faced with the curious situation that the disordered state has the density of the liquid and the coordination of the solid. This state is, however, only a transient in the melting process. The second stage of melting involves a change in the atomic coordination to produce a fully isotropic liquid state.

IV. SURFACE-INDUCED MELTING

Melting of silicon surfaces has been studied by simulation under a variety of conditions.[17,37,46] Our interest in surface-induced melting is mainly to obtain results on the kinetics of melting that can be compared with the GB study in order to draw conclusions having more general implications.

We simulated surface-induced melting at four temperatures: 1900, 2000, 2100, and 2200 K. At 1900 K nucleation of melting takes approximately 10 000 time steps, as compared with only $\approx$3000 time steps in the GB at the same temperature. Because of this long nucleation time, no attempt was made to simulate surface-induced melting at temperatures below 1900 K. As the temperature is increased this difference between nucleation times at the free surface and at the GB decreases such that it is found to be negligible at 2100 K.

The inequality in nucleation times can be attributed to the inherently different degrees of disorder in the GB and on the surface, as evidenced by the related radial and angular distribution functions (not shown). For the SW potential, there is a high degree of disorder at the interface in the bicrystal. In contrast, the disorder on the (110) free surface arises only from the loss of one nearest neighbor by atoms on the surface layer. We believe that this is the reason that the nucleation time is longer for the free surface.

Despite the longer nucleation time our simulations are long enough to observe significant melting at all four tem-

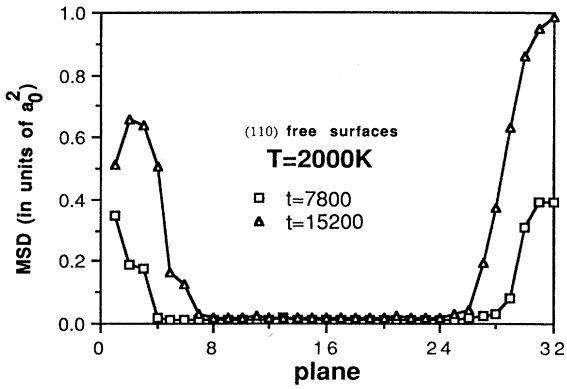

FIG. 12. Instantaneous mean-square-displacement profile after 7800 and 15 200 time steps at 2000 K for surface-induced melting.

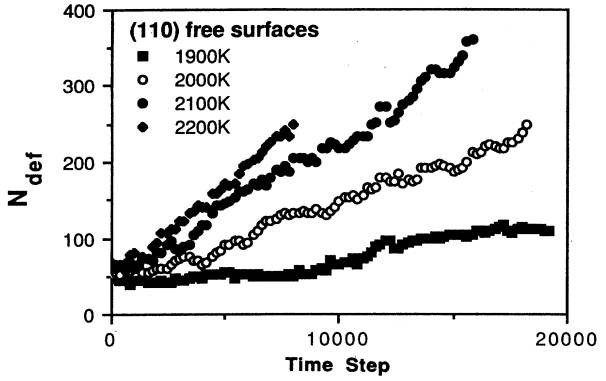

FIG. 13. Number of defected atoms as a function of time for four temperatures during surface-induced melting.

peratures. The behavior of the structure factor, MSD and N_{def} were similar over this temperature range. Figure 11 shows the instantaneous planar structure factor after 7800 and 15 200 time steps at 2000 K. It is clear that a disordered region is spreading from the surface into the bulk. This disordering is also evident in the MSD profile, shown in Fig. 12 at the same to instants. Again this disordered region is identified to be liquid on the basis of the diffusion constant, which is determined to be $\approx 1.2\times 10^{-8}$ m^2/s at 2000 K, a value comparable to that of the bulk liquid.[35]

Figure 13 shows N_{def} as a function of time for the four temperatures studied. There is a clear linear increase in the number of defected atoms with time, and propagation velocities may be extracted (Table I). For the three temperatures at which simulations were performed for both the surface and the GB, we find that the velocity is the same for both. The implication is that, after the initial nucleation, the melting behaviors are the same. This is consistent with our interpretation in Sec. III that the melting observed is ordinary thermodynamic melting.

V. CONCLUSIONS

In this paper we have presented molecular-dynamics results on the characteristics of melting in Si initiated at a high-angle twist grain boundary and at a (110) free surface at temperatures above the thermodynamic melting point T_m associated with the SW potential. By using different ways of determining the growth of the melt and by extrapolating the various growth rates to zero velocity of propagation, we have shown that the extrapolated temperature is in agreement with T_m as determined by free-energy calculations.[35] The choice of an interatomic potential with a known thermodynamic melting point and the use of crystal configurations with and without an extrinsic surface have enabled us to explicitly demonstrate the connection between melting, in the thermodynamic definition in terms of the free energies, and melting when the system is superheated.

The major conclusion from this work is that nucleation at an extrinsic surface is the predominant mechanism of melting, since other possible mechanisms, involving lattice instability or spontaneous generation of defects, either do not occur by thermal activation alone or have slower kinetics. This conclusion, which, as discussed in the Introduction, is entirely in accord with experiment, leads us to question the relevance of theories of melting that are based on thermal generation of defects.

Our results also show that when an extrinsic surface is absent, as is the case of a perfect-crystal model with 3D periodic borders, the upper limit of superheating is the point at which the lattice loses its mechanical stability, a process that is readily observed by simulation. These findings are fully consistent with a separate study, presented in the following paper, of an fcc metal for which the potential function and crystal structure are quite different from silicon (paper II). This consistency is important not only for the wider validity of the conclusions, but also for demonstrating that our border condition (Sec. II A and Ref. 40) and method of data analysis are generally useful. The observation that superheating is impossible, except in the absence of extrinsic surfaces, is consistent with the experiments discussed in the Introduction.

From our investigation, it appears essential to know the thermodynamic melting temperature associated with a given potential, in order to understand the high-temperature behavior found in its applications. Indeed, we believe that the important distinction between the thermodynamic melting temperature, T_m, and the mechanical melting temperature, T_s, has not been fully appreciated in the simulation literature. It appears that phenomena previously believed to occur below the temperature at which the bulk melts, may actually have occurred above T_m. Calculating T_m by free-energy analysis is a time consuming and technically difficult process, as is illustrated in Paper II. We note that extrapolation of solid-liquid interface velocities to zero provides a convenient operational way of obtaining T_m.

As to the question of premelting, our results on the (110) twist bicrystal show that this grain boundary with a large spacing of lattice planes parallel to the GB plane is quite stable in silicon up to temperatures close to the thermodynamic melting point. That this, in fact, holds in general is strongly suggested by the corresponding results obtained on a (100) twist boundary in Cu (Paper II).

We have studied the free surface here in order to show that different kinds of extrinsic surfaces can provide nucleation sites for the initiation of thermodynamic melting. It should be noted that the melting behavior of free surfaces of Si is a problem of considerable current interest in its own right.[17,46,50] Simulation of laser-pulse melting of (100) and (111) surfaces has shown quite different interfacial characteristics.[17] Also a recent careful study of crystallization and melting at the (100) surface gives propagation velocities showing the proper asymmetry between the two processes.[46] Our data on the propagation velocity on melting (i.e., above T_m) are in reasonable agreement with these results.

Finally, to our knowledge this is the first simulation where the effects of an internal interface and a free surface are explicitly compared. It seems that other studies of interfacial properties can usefully exploit the commonality of these two systems.

ACKNOWLEDGMENTS

We are indebted to Professor H. Gleiter for several helpful suggestions and discussions. This work was supported by the U. S. Department of Energy, Office of Basic Energy Sciences, Materials Science, under Contract No. W-31-109-Eng-38. The authors wish to acknowledge a grant of computer time at the Energy Research CRAY XMP at the Magnetic Fusion Computational Center at Livermore.

---

*Permanent address: Department of Nuclear Engineering, Massachusetts Institute of Technology, Cambridge, MA 02139.

[1]A. R. Ubbelohde, *Molten State of Matter: Melting and Crystal Structure* (Wiley, Chichester, 1978).

[2]L. L. Boyer, Phase Transitions **5**, 1 (1985).

[3]R. M. J. Cotterill, J. Cryst. Growth **48**, 582 (1980).

[4]R. W. Cahn, Nature **273**, 491 (1978).

[5]N. G. Ainslie, J. D. Mackenzie, and D. Turnbull, J. Phys. Chem. **65**, 1718 (1961).

[6]R. L. Cormia, J. D. Mackenzie, and D. Turnbull, J. Appl. Phys. **34**, 2239 (1963).

[7]R. W. Cahn, Nature **323**, 668 (1986).

[8]Ph. Buffat and J.-P. Borel, Phys. Rev. A **13**, 2287 (1976).

[9]J. B. Boyce and M. Stutzmann, Phys. Rev. Lett. **54**, 562 (1985).

[10]C. J. Rossouw and S. E. Donnelly, Phys. Rev. Lett. **55**, 2960 (1985).

[11]J. Daeges, H. Gleiter, and J. H. Perepezko, Phys. Lett. **119A**, 79 (1986).

[12]See, for example, *Simulations of Liquids and Solids,* edited by G. Ciccotti, D. Frenkel, and I. R. McDonald (North-Holland, Amsterdam, 1987); *Molecular Dynamics Simulation of Statistical Mechanical Systems,* edited by G. Ciccotti and W. G. Hoover (North-Holland, Amsterdam, 1985).

[13]*Monte Carlo Methods in Statistical Physics,* edited by K. Binder (Springer-Verlag, Berlin, 1979).

[14]D. Frenkel and J. P. McTague, Ann. Rev. Phys. Chem. **31**, 491 (1980).

[15]J. R. Fox and H. C. Andersen, J. Phys. Chem. **88**, 4019 (1984).

[16]R. M. J. Cotterill, Philos. Mag. **32**, 1283 (1975); F. F. Abraham, Phys. Rev. B **23**, 6145 (1981); J. Q. Broughton and G. Gilmer, J. Chem. Phys. **79**, 5105, 5119 (1983), Acta Metall. **31**, 845 (1983); W. Schommers and P. von Banckenhagen, Vacuum **33**, 733 (1983), Surf. Sci. **162**, 144 (1985); V. Pontikis and V. Rosato, Surf. Sci. **162**, 150 (1985); V. Rosato, G. Ciccotti, and V. Pontikis, Phys. Rev. B **33**, 1860 (1986).

[17]F. F. Abraham and J. Q. Broughton, Phys. Rev. Lett. **56**, 734 (1986).

[18]P. Stoltze, J. K. Norskov, and U. Landman, Phys. Rev. Lett. **61**, 440 (1988).

[19]J. W. M. Frenken, P. M. Maree, and J. F. van der Veen, Phys. Rev. B **34**, 7506 (1986).

[20]R. Lipowsky and W. Speth, Phys. Rev. B **28**, 3983 (1983); R. Lipowsky, J. Appl. Phys. **55**, 2485 (1984).

[21]K. T. Aust, in *Progress in Materials Science, Chalmers Anniversary Volume,* edited by J. W. Christian, P. Haasen, and T. B. Massalski (Pergamon, Oxford, 1981), p. 27; E. W. Hart, in *The Nature and Behavior of Grain Boundaries,* edited by P. Hu (Plenum, New York, 1972), p. 155.

[22]G. Ciccotti, M. Guillope, and V. Pontikis, Phys. Rev. B **27**, 5576 (1983); M. Guillope, G. Ciccotti, and V. Pontikis, Surf. Sci. **144**, 67 (1984).

[23]F. Carrion, G. Kalonji, and S. Yip, Scripta Met. **17**, 915 (1983); P. Deymier, G. Kalonji, R. Najafabadi, and S. Yip, Surf. Sci. **144**, 77 (1984).

[24]P. S. Ho, T. Kwok, T. Nguyen, C. Nitta, and S. Yip, Scripta Met. **19**, 993 (1985); T. Nguyen, P. S. Ho, T. Kwok, C. Nitta, and S. Yip, Phys. Rev. Lett. **57**, 1919 (1986).

[25]P. Deymier and G. Kalonji, Trans. Jpn. Inst. Metals Suppl. **27**, 171 (1986).

[26]J. Q. Broughton and G. H. Gilmer, Phys. Rev. Lett. **56**, 2692 (1986).

[27]U. Erb and H. Gleiter, Scripta Met. **13**, 61 (1979).

[28]R. W. Balluffi and R. Maurer, Scripta Met. **22**, 709 (1988).

[29]S. W. Chan, J. L. Liu, and R. Balluffi, Scripta Met. **19**, 1251 (1985).

[30]R. W. Balluffi and T. S. Hsieh, J. Phys. (Paris) Colloq. **49**, C5-337 (1988).

[31]J. F. Lutsko, D. Wolf, S. R. Phillpot, and S. Yip, following paper, Phys. Rev. B **40**, 2841 (1989).

[32]J. F. Lutsko and D. Wolf (unpublished).

[33]D. A. Smith and T. Y. Tan, in *Grain Boundaries in Semiconductors,* edited by H. J. Leamy, G. E. Pike, and C. H. Seeger (North-Holland, Amsterdam, 1982).

[34]F. H. Stillinger and T. A. Weber, Phys. Rev. B **31**, 5262 (1985).

[35]J. Q. Broughton and X. P. Li, Phys. Rev. B **35**, 9120 (1987).

[36]U. Landman, W. D. Leudtke, R. Barnett, C. L. Cleveland, M. W. Ribarsky, E. Arnold, S. Ramesh, H. Baumgart, A. Martinez, and B. Kahn, Phys. Rev. Lett **56**, 155 (1986).

[37]U. Landman, W. D. Luedtke, M. W. Ribarsky, R. N. Barnett, and C. L. Cleveland, Phys. Rev. B **37**, 4637 (1988); W. D. Luedtke, U. Landman, M. W. Ribarsky, R. N. Barnett, and C. L. Cleveland, *ibid.* **37**, 4647 (1988).

[38]S. R. Phillpot and D. Wolf, in *Interfacial Structure, Properties and Design,* Vol. 122 of *Materials Research Society Symposium Proceedings,* edited by M. H. Yoo, W. A. T. Clark, and C. L. Briant (MRS, Pittsburgh, PA, 1988), p. 129; S. R. Phillpot and D. Wolf, Philos. Mag. A (to be published).

[39]S. R. Phillpot, J. F. Lutsko, and D. Wolf, Solid State Commun. **70**, 265 (1989).

[40]J. F. Lutsko, D. Wolf, S. Yip, S. R. Phillpot, and T. Nguyen, Phys. Rev. B **38**, 11 572 (1988).

[41]D. Wolf, J. Am. Cer. Soc. **67**, 1 (1984).

[42]D. Wolf, in *Computer Simulations in Materials Science,* edited by R. J. Arsenault, J. R. Beeler, and D. M. Esterling (ASM, Metals Park, Ohio, 1987), p. 111.

[43]M. Parrinello and A. Rahman, J. Appl. Phys. **52**, 7182 (1981).

[44]J. Tersoff, Phys. Rev. Lett. **56**, 632 (1986).

[45]R. Biswas and D. R. Hamann, Phys. Rev. Lett. **55**, 2001 (1985).

[46]M. I. Baskes, Phys. Rev. Lett. **59**, 2666 (1987).

[47]B. P. Feuston, R. K. Kalia, and P. Vashishta, Phys. Rev. B **35**, 6222 (1987).

[48]W. D. Luedtke and U. Landman, Phys. Rev. B **37**, 4656 (1988).

[49]M. D. Kluge and J. R. Ray, Phys. Rev. B **39**, 1738 (1989).

[50]J. Y. Tsao, M. J. Aziz, M. O. Thompson, and P. S. Peercy, Phys. Rev. Lett. **56**, 2712 (1986).